Electrical conductivity in sprite streamer channels

F. J. Gordillo-Vázquez[1] and A. Luque[1]

Received 21 June 2010; revised 12 July 2010; accepted 20 July 2010; published 25 August 2010.

[1] We study the electrical conductivity of a sprite streamer channel at three different altitudes (63 km, 70 km and 80 km). We discuss the hypothesis that the electrical conductivity stays constant along the full length of a streamer channel, contrary to expectations based on scaling laws. We then apply this hypothesis and extrapolations from a numerical electrodynamical simulation to study the air plasma kinetics after the passage of a streamer. We test two possible scenarios for the physical origin of trailing sprite emissions: a single pulse and a single pulse with a delayed re-enhancement of the electric field up to the breakdown value. Our simulations show that VLF observations agree with persistent electric fields in the sprite that last several milliseconds and that associative detachment of O^- ions may significantly affect the atmospheric conductivity in the presence of sprites.
Citation: Gordillo-Vázquez, F. J., and A. Luque (2010), Electrical conductivity in sprite streamer channels, *Geophys. Res. Lett.*, *37*, L16809, doi:10.1029/2010GL044349.

1. Introduction

[2] Sprites are transient luminous events observed in the mesosphere and lower ionosphere. First reported in 1990 [*Franz et al.*, 1990], they are usually caused by a positive cloud-to-ground lightning stroke with a large charge moment change [*Boccippio et al.*, 1995]. Recent telescopic [*Gerken et al.*, 2000] and high-speed [*Cummer et al.*, 2006; *McHarg et al.*, 2007; *Stenbaek-Nielsen and McHarg*, 2008] sprite observations clarify the nature of sprites and their underlying physics. Sprites exhibit a highly nonuniform altitude structure characterized by a lower (approximately 50–80 km) streamer-like region and a higher (approximately 80–90 km) diffuse glow region. Sprite streamers [*Pasko et al.*, 1996] are thin channels of ionized air that propagate due to the enhanced electric field at their tip [*Ebert et al.*, 2006]. In a sprite, streamers always start propagating downwards [*Stenbaek-Nielsen and McHarg*, 2008], sometimes shooting out from a diffuse halo [*Barrington-Leigh et al.*, 2001; *Cummer et al.*, 2006; *Luque and Ebert*, 2009] and propagating at speeds of $\sim 10^7$ m/s [*McHarg et al.*, 2007; *Stenbaek-Nielsen and McHarg*, 2008]. Sometimes, upward-propagating streamers emerge later from previous channels as observed, e.g., by *Stenbaek-Nielsen and McHarg* [2008] producing "carrot" sprites.

[3] Sprites are known to affect the atmospheric electric conductivity: this is the reason that sprites very efficiently scatter sub-ionospheric VLF waves (electromagnetic waves in the 3–30 kHz frequency range), generating a very clear signature in VLF detectors termed "VLF sprite" [*Inan et al.*, 1995; *Dowden and Rodger*, 1997; *Rodger and McCormick*, 2006]. *Dowden et al.* [2001] applied measurements of wide-angle VLF scattering to set an approximate lower bound for plasma conductivities in a sprite to about $3 \cdot 10^{-7}$ mho/cm. The VLF measurements by *Dowden et al.* [2001] were carried out in the millisecond time scale and, therefore, the lower bound of $3 \cdot 10^{-7}$ mho/cm for sprite plasmas applies to the millisecond time scale. The conductivity tens of milliseconds after the passage of the streamer heads might be much smaller because of the small values of the reduced electric fields just after the passage of the initial pulse exciting the sprite. A similar value to the conductivity reported by *Dowden et al.* [2001] is also given by *Williams et al.* [2006], who used a laboratory glow-discharge tube to calibrate electrical conductivity as a function of the absolute radiance of the first positive system of N_2 emitted from sprites. At 70 km the conductivity derived by *Williams et al.* [2006], corresponds to a numerical electron density of about $3 \cdot 10^{11}$ m^{-3}. The latest sprite simulations by *Liu et al.* [2009] and, extrapolated, by *Luque and Ebert* [2010] predict lower conductivities of about $8 \cdot 10^{-8}$ mho/cm and $5 \cdot 10^{-8}$ mho/cm, respectively.

[4] In this paper, we use the detailed atmospheric kinetic model of *Gordillo-Vázquez* [2008] with electric field data extracted from the self-consistent electrodynamic simulations using realistic altitude-dependent air densities performed by *Luque and Ebert* [2010]. Our focus is to study the variation of the atmospheric conductivity on a relatively long timescale of milliseconds or tens of milliseconds, relevant for VLF observations. These changes in the conductivity of the upper atmosphere affect also the circulation of charges between the Earth's surface and the ionosphere inside the so-called global electrical circuit. We provide modelling predictions based on two alternative models for the variation of electric fields inside streamer channels in the millisecond time-scale.

2. Model

2.1. Kinetic Model

[5] Air plasma kinetics is modelled here as discussed by *Gordillo-Vázquez* [2008, 2010]: a zero-dimensional model that solves a set of differential rate equations for each of the chemical species in the streamer plasma coupled to a time-dependent Boltzmann equation for the electron energy distribution function with a prescribed time-dependent electric field.

2.2. Constant Conductivity Along the Streamer Channel

[6] Townsend scaling [*Ebert et al.*, 2010], if applied naively, predicts that as a sprite streamer propagates into regions with higher air density N, the electron density scales as $\sim N^2$ and therefore the channel conductivity is larger at

[1]Instituto de Astrofísica de Andalucía, CSIC, Granada, Spain.

0094-8276/10/2010GL044349

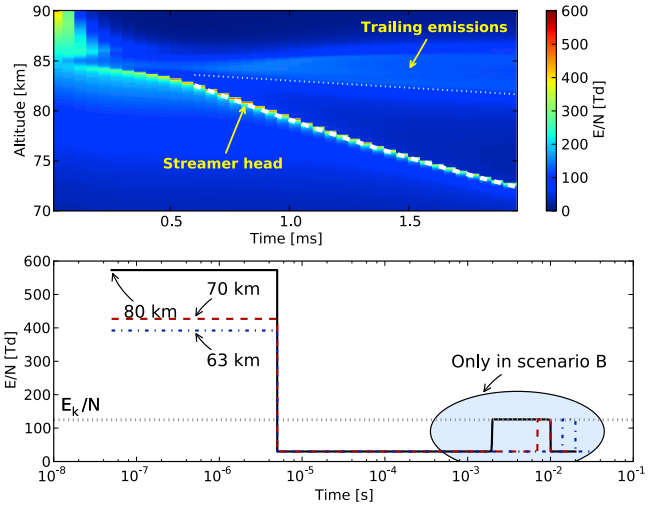

Figure 1. Modeling of electric fields. (top) Reduced electric field E/N calculated in the self-consistent simulations for the first 2 ms of streamer propagation and fits to the streamer head altitude and lower edge of the trailing emissions. The fits are, respectively $z_{head} = a_0 + a_1 t + a_2 t^2$ with $(a_0, a_1, a_2) = (88.5\text{ km}, -1.05 \cdot 10^7\text{ m/s}, 1.2 \cdot 10^9\text{ m/s}^2)$ and $z_{trail} = b_0 + b_1 t$ with $(b_0, b_1) = (88.5\text{ km}, -1.4 \cdot 10^6\text{ m/s})$. (bottom) Electric fields used in scenarios A and B in the kinetic model at three different altitudes (63 km, 70 km, 80 km). The intensity of the first pulse is the same as in the self-consistent model at 80 km and matches the same conductivity in the wake of the pulse at 70 km and 63 km. The height of the second pulse is always E_k/N. The delay between both pulses at 80 and 70 km is obtained from the fit detailed above. At 63 km, where the fit is not meaningful, we used a reasonable but arbitrary delay of 15 ms. We provide simulations at that altitude only for comparison.

lower altitudes (electron mobility scales as $\sim 1/N$). However the electron density is selected dynamically as the streamer propagates downwards and thus Townsend scaling does not apply. As by *Luque and Ebert* [2010] for the first time a numerical model for sprites included the variation in air density and it showed that the electron density is roughly proportional to N and therefore the conductivity is constant along the streamer propagation length. This approximation may arise from a power expansion of the electron density as a function of N with the linear term being dominant.

[7] Note that the above finding maybe connected to the logarithmic decay of VLF perturbations as discussed by *Dowden and Rodger* [1997], suggesting a roughly constant conductivity along the full sprite height. However, VLF waves probe the atmospheric conductivity only on timescales of the order of milliseconds. As we discuss later, it is possible that VLF perturbations arise from changes in the conductivity induced by a delayed increase in the electric field.

[8] In this paper we work under the assumption that the enhanced electric field at the streamer tip is adjusted in such a manner that the electrical conductivity immediately behind is constant along the full propagation length. We then obtain the full time-dependence of the streamer chemical properties from the detailed chemical model of *Gordillo-Vázquez* [2008, 2010].

2.3. Electric Fields

[9] In high-speed optical observations, sprite streamers show a glowing region in the streamer trail [*Stanley et al.*, 1999; *McHarg et al.*, 2007; *Stenbaek-Nielsen and McHarg*, 2008]. Some authors [*Kanmae et al.*, 2007; *Sentman et al.*, 2008] attributed it to the release of energy stored in the vibrational levels of N_2 during the passage of the streamer head. However, spectroscopical observations by *Morrill et al.* [2002], altitude-resolved optical observations by *Stenbaek-Nielsen et al.* [2010] and two recent modelling papers by *Liu* [2010] and *Luque and Ebert* [2010] have made it increasingly clear that the glowing trails arise from a trailing enhanced electric field close to the breakdown value E_k/N and the subsequent collisional excitation of molecular nitrogen.

[10] *Luque and Ebert* [2010] explain this field as arising from the upward drift inside the streamer channel of an exponentially increasing number of electrons liberated around the streamer head. These drifting electrons at some point surpass the local number of positive ions and create a negative charge and an increase in the electric field. A compatible explanation is given by *Liu* [2010]: the field increases in order to keep the total current constant along the streamer length.

[11] Here we analyze two alternative scenarios (see Figure 1) for the origin of the trailing emissions and investigate how they would affect the atmospheric conductivity. In our scenario A, the electric field is modelled as a single 5 μs pulse; in scenario B, the electric field has a second, long-lasting pulse between 2 ms (80 km) and 15 ms (63 km) after the initial one. Each scenario is then applied to three altitudes: 80 km, 70 km and 63 km.

[12] The self-consistent transport model can follow the propagation of a streamer for about 2 ms (about 10 km). At that time, the limited spatial resolution generates numerical artifacts and produces unreliable results. Furthermore, it is well known from direct optical observations that streamers branch after similar distances. Our approach therefore is to extrapolate the propagation of the first 2 ms to longer times (i.e., lower altitudes).

[13] As discussed above, in both scenarios A and B, the height of the first pulse, modeling the passage of a streamer head, is adjusted to leave the same conductivity immediately afterwards. We take the highest electric field at 80 km from the simulations of *Luque and Ebert* [2010], where a streamer shoots from a halo-like steep change in the conductivity at 85 km. The electric fields at 70 km and 63 km were obtained from the kinetic model of *Gordillo-Vázquez* [2008] after imposing approximately the same conductivity value as that obtained at 80 km.

[14] To estimate the delay between the two pulses in scenario B, we fitted the position of the streamer head and the lower edge of the trailing emissions in the simulations with, respectively, a quadratic and a linear dependence on time. The result of this fit is displayed in Figure 1 (top). The reduced electric field during the second pulse is always $E/N = E_k/N$. The resulting time-dependent electric fields are plotted in Figure 1.

3. Results

[15] Figure 2 shows the contributions to the total electrical conductivity of the most relevant negative species for both scenarios. In both scenarios, the electronic conductivity is

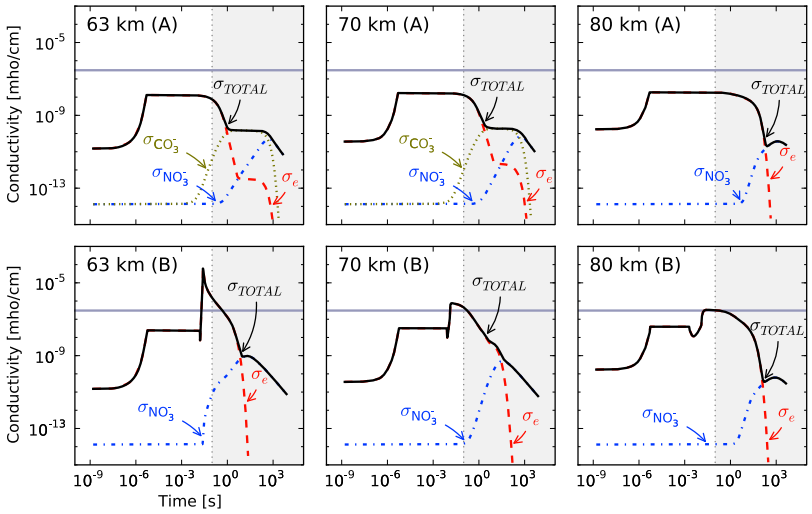

Figure 2. Contribution of the negative species to the plasma conductivity at the streamer axis for scenario (top) A (single pulse) and (bottom) B (pulse + re-enhancement of the electric field). The shaded area (at 100 ms) to the right of each panel indicates the approximate end of optical emissions. The horizontal gray line corresponds to a conductivity of $3 \cdot 10^{-7}$ mho/cm as reported by *Dowden et al.* [2001] in the millisecond time scale and by *Williams et al.* [2006] in steady state DC discharges in air.

the main contributor to the total conductivity up to several seconds. For longer times, negative ions (mainly NO_3^- and CO_3^-) replace electrons. In scenario A (Figure 2, top), the contribution of NO_3^- is important at very long times while that of CO_3^- only plays a distinct role at 63 km and 70 km. In scenario B (Figure 2, bottom), electrons and O_3^- ions are the most important contributors to the value of the total conductivity.

[16] The most remarkable feature shown in Figure 2 (scenario B) is the sudden increase in the millisecond time range of the total conductivity as a consequence of the second pulse with a reduced electric field of $E/N = E_k/N$. The second jump in the total conductivity is more pronounced for lower altitudes and goes from a peak value of almost $1 \cdot 10^{-4}$ mho/cm at 63 km to $4 \cdot 10^{-7}$ mho/cm at 80 km.

[17] We note that the conductivity in the wake of the first pulse is lower than the value estimated by *Dowden et al.* [2001] in the millisecond time range and by *Williams et al.* [2006] in steady state DC discharges in air. In scenario B, however, the second pulse creates a much larger conductivity in the millisecond time scale that, according to *Dowden et al.* [2001] would scatter a VLF signal efficiently enough to produce the observed signature of VLF sprites. Although this topic needs to be investigated further, this may be an indirect experimental evidence that there is a re-enhancement of the electric field, as modelled in scenario B.

[18] At 63 km, the conductivity resulting from scenario B is too large: the associated Maxwell relaxation time would make the electric field decay much faster than what we assumed in the model. To our knowledge there are no distinct observations of trailing emissions separated from the streamer head by distances longer than about 15 km. We give these results for comparison and completeness. Note, however, that the highest conductivities at 70 km and 80 km are similar within a factor of about 3. This is consistent with a constant conductivity in the millisecond timescale, as suggested by *Dowden et al.* [2001].

[19] During the first and second pulse, the most important positive ions responsible for keeping the charge neutrality in the streamer plasma are $N_2O_2^+$ and NO^+. The concentration of $N_2O_2^+$ is always above that of NO^+ except at 63 km for times beyond 500 miliseconds. This is consistent with previous results by *Gordillo-Vázquez* [2008] but differs from predictions by *Sentman et al.* [2008] for 70 km where O_2^+ prevails over NO^+ and $N_2O_2^+$ up to 100 milliseconds, when the concentration of $N_2O_2^+$ becomes dominant.

[20] The kinetic mechanisms underlying the sharp increase of CO_3^- and NO_3^- are $O_3^- + CO_2 \rightarrow CO_3^- + O_2$ (for CO_3^-) and $CO_3^- + NO_2 \rightarrow NO_3^- + CO_2$ (for NO_3^-). The latter is true for both scenarios considered at 70 km and 80 km, while at 63 km, the mechanism controling the growth of the concentration of NO_3^- is $NO_2^- + O_3 \rightarrow O_2 + NO_3^-$ in scenario B and $CO_3^- + NO_2 \rightarrow NO_3^- + CO_2$ in scenario A. The most important processes underlying the formation of the negative ions CO_3^- and NO_3^- are the same predicted by *Gordillo-Vázquez* [2008] and *Sentman et al.* [2008].

[21] As mentioned above, the sudden increase of the total conductivity in the first and second jumps in scenarios A and B shown in Figure 2 is due to the sharp increase in both cases of the electronic conductivity. In this regard, the kinetic mechanisms controling the concentration of electrons in sprite streamer heads at all altitudes considered are electron impact ionization of N_2 and O_2 in scenario A and associative detachment $O^- + N_2 \rightarrow N_2O + e$ in scenario B (see Figure 3 (bottom) for the case of 63 km). In addition, as can be seen in Figure 3 (top), associative detachment becomes more important at lower altitudes. While the rates of electron impact ionization of N_2 and O_2 exhibit a sharp decrease (around 30 ms at 63 km), the rate of associative detachment has a smooth decrease which explains the scenario B shape of the electronic (and total) conductivity up to around 10 seconds. Associative dettachment of O^- by N_2 ($O^- + N_2 \rightarrow N_2O + e$) was earlier discussed by *Gordillo-Vázquez* [2008] as the main mechanism responsible for the

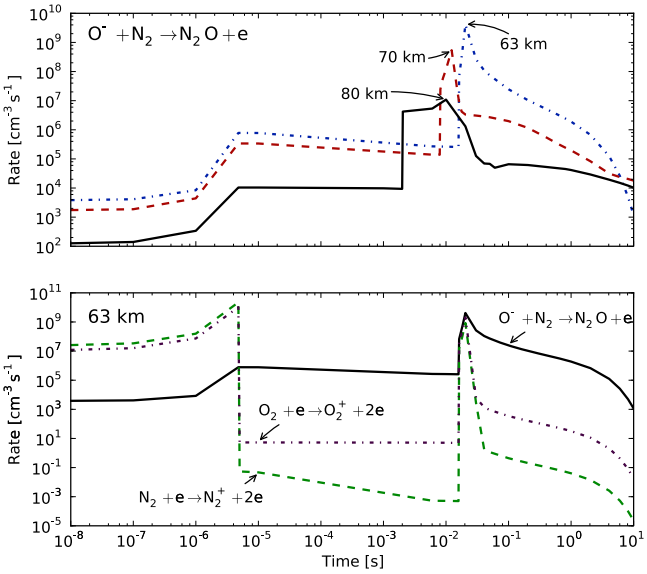

Figure 3. Rates of the most relevant electron production mechanisms in our scenario B. (top) Rates of production of electrons through fast associative detachment at three different altitudes. (bottom) Comparison of the three most relevant mechanisms of electron production at 63 km. During the passage of the streamer head, impact ionization of N_2 and O_2 dominates strongly but for longer times, fast detachment from O^- becomes the most relevant source of electrons.

loss of O^- ions in sprite streamers; however, the kinetic model of *Sentman et al.* [2008] did not include this mechanism in its kinetic scheme although some other associative dettachment processes (also included in the kinetic model by *Gordillo-Vázquez* [2008]) were considered.

[22] The large increase in conductivity induced by associative detachment would in turn significantly affect the dynamics of a self-consistent model in long time-scales. To our knowledge, no self-consistent, electrodynamic sprite streamer models have yet included the production of O^- in the streamer head and the subsequent detachment of electrons in the streamer channel. However, our model, in combination with the increase in the channel electric field predicted by *Liu* [2010] and *Luque and Ebert* [2010] shows that associative detachment is crucial to understanding the sprite dynamics on the milliseconds to hundreds-of-millisecond scale. Future models aimed to study sprites on those scales should take it into account.

4. Summary and Conclusions

[23] We have used a detailed chemical model and inputs from a self-consistent model to study the conductivity of sprite streamers on timescales of 10^{-6}–10^{-1} s. Our results provide further support to the interpretation of the trailing luminosity in streamers as resulting from a electric field $E \sim E_k$. We also noted the relevance of fast associative detachment of electrons from O^- ions by N_2 as the dominant contributor to the production of electrons inside the streamer channel.

[24] Our model shows that sprite-induced changes in the atmospheric conductivity last for several minutes after the discharge, long after optical emissions can be detected. This agrees with previous observation of sprite reignition events [*Stenbaek-Nielsen et al.*, 2000]. Those long-lasting changes are enhanced in our scenario B and should be taken into account to study the influence of sprites on the global electrical circuit. The presence of fields $E \sim E_k$ lasting a few milliseconds to tens of milliseconds also has implications for the atmospheric chemistry induced by sprites.

[25] **Acknowledgments.** This work was supported by the Spanish Ministry of Science and Innovation, MICINN under project AYA2009-14027-C05-02.

References

Barrington-Leigh, C. P., U. S. Inan, and M. Stanley (2001), Identification of sprites and elves with intensified video and broadband array photometry, *J. Geophys. Res.*, *106*, 1741, doi:10.1029/2000JA000073.

Boccippio, D. J., E. R. Williams, S. J. Heckman, W. A. Lyons, I. T. Baker, and R. Boldi (1995), Sprites, ELF transients, and positive ground strokes, *Science*, *269*, 1088, doi:10.1126/science.269.5227.1088.

Cummer, S. A., N. Jaugey, J. Li, W. A. Lyons, T. E. Nelson, and E. A. Gerken (2006), Submillisecond imaging of sprite development and structure, *Geophys. Res. Lett.*, *33*, L04104, doi:10.1029/2005GL024969.

Dowden, R. L., and C. J. Rodger (1997), Decay of a vertical plasma column: A model to explain VLF sprites, *Geophys. Res. Lett.*, *24*, 2765, doi:10.1029/97GL02822.

Dowden, R. L., C. J. Rodger, and D. Nunn (2001), Minimum sprite plasma density as determined by VLF scattering, *IEEE Trans. Antennas Propag.*, *43*, 12, doi:10.1109/74.924600.

Ebert, U., C. Montijn, T. M. P. Briels, W. Hundsdorfer, B. Meulenbroek, A. Rocco, and E. M. van Veldhuizen (2006), The multiscale nature of streamers, *Plasma Sour. Sci. Technol.*, *15*, 118, doi:10.1088/0963-0252/15/2/S14.

Ebert, U., S. Nijdam, C. Li, A. Luque, T. Briels, and E. van Veldhuizen (2010), Review of recent results on streamer discharges and discussion of their relevance for sprites and lightning, *J. Geophys. Res.*, *115*, A00E43, doi:10.1029/2009JA014867.

Franz, R. C., R. J. Nemzek, and J. R. Winckler (1990), Television image of a large upward electrical discharge above a thunderstorm system, *Science*, *249*, 48, doi:10.1126/science.249.4964.48.

Gerken, E. A., U. S. Inan, and C. P. Barrington-Leigh (2000), Telescopic imaging of sprites, *Geophys. Res. Lett.*, *27*, 2637, doi:10.1029/2000GL000035.

Gordillo-Vázquez, F. J. (2008), Air plasma kinetics under the influence of sprites, *J. Phys. D*, *41*(23), 234016, doi:10.1088/0022-3727/41/23/234016.

Gordillo-Vázquez, F. J. (2010), Vibrational kinetics of air plasmas induced by sprites, *J. Geophys. Res.*, *115*, A00E25, doi:10.1029/2009JA014688.

Inan, U. S., T. F. Bell, V. P. Pasko, D. D. Sentman, E. M. Wescott, and W. A. Lyons (1995), VLF signatures of ionospheric disturbances associated with sprites, *Geophys. Res. Lett.*, *22*, 3461, doi:10.1029/95GL03507.

Kanmae, T., H. C. Stenbaek-Nielsen, and M. G. McHarg (2007), Altitude resolved sprite spectra with 3 ms temporal resolution, *Geophys. Res. Lett.*, *34*, L07810, doi:10.1029/2006GL028608.

Liu, N. (2010), Model of sprite luminous trail caused by increasing streamer current, *Geophys. Res. Lett.*, *37*, L04102, doi:10.1029/2009GL042214.

Liu, N. Y., V. P. Pasko, K. Adams, H. C. Stenbaek-Nielsen, and M. G. McHarg (2009), Comparison of acceleration, expansion, and brightness of sprite streamers obtained from modeling and high-speed video observations, *J. Geophys. Res.*, *114*, A00E03, doi:10.1029/2008JA013720.

Luque, A., and U. Ebert (2009), Emergence of sprite streamers from screening-ionization waves in the lower ionosphere, *Nat. Geosci.*, *2*, 757, doi:10.1038/ngeo662.

Luque, A., and U. Ebert (2010), Sprites in varying air density: Charge conservation, glowing negative trails and changing velocity, *Geophys. Res. Lett.*, *37*, L06806, doi:10.1029/2009GL041982.

McHarg, M. G., H. C. Stenbaek-Nielsen, and T. Kammae (2007), Observations of streamer formation in sprites, *Geophys. Res. Lett.*, *34*, L06804, doi:10.1029/2006GL027854.

Morrill, J., et al. (2002), Electron energy and electric field estimates in sprites derived from ionized and neutral N_2 emissions, *Geophys. Res. Lett.*, *29*(10), 1462, doi:10.1029/2001GL014018.

Pasko, V. P., U. S. Inan, and T. F. Bell (1996), Sprites as luminous columns of ionization produced by quasi-electrostatic thundercloud fields, *Geophys. Res. Lett.*, *23*, 649, doi:10.1029/96GL00473.

Rodger, C. J., and R. J. McCormick (2006), Remote sensing of the upper atmosphere by VLF, in *Sprites, Elves and Intense Lightning Discharges*, *NATO Sci. Ser., Ser. II*, vol. 225, edited by M. Füllekrug, E. A. Mareev, and M. J. Rycroft, p. 237, Springer, Dordrecht, Netherlands.

Sentman, D. D., H. C. Stenbaek-Nielsen, M. G. McHarg, and J. S. Morrill (2008), Plasma chemistry of sprite streamers, *J. Geophys. Res.*, *113*, D11112, doi:10.1029/2007JD008941.

Stanley, M., P. Krehbiel, M. Brook, C. Moore, W. Rison, and B. Abrahams (1999), High speed video of initial sprite development, *Geophys. Res. Lett.*, *26*, 3201, doi:10.1029/1999GL010673.

Stenbaek-Nielsen, H. C., and M. G. McHarg (2008), High time-resolution sprite imaging: Observations and implications, *J. Phys. D*, *41*(23), 234009, doi:10.1088/0022-3727/41/23/234009.

Stenbaek-Nielsen, H. C., D. R. Moudry, E. M. Wescott, D. D. Sentman, and F. T. S. Sabbas (2000), Sprites and possible mesospheric effects, *Geophys. Res. Lett.*, *27*, 3829, doi:10.1029/2000GL003827.

Stenbaek-Nielsen, H. C., R. Haaland, M. G. McHarg, B. A. Hensley, and T. Kanmae (2010), Sprite initiation altitude measured by triangulation, *J. Geophys. Res.*, *115*, A00E12, doi:10.1029/2009JA014543.

Williams, E., M. Valente, E. Gerken, and R. Golka (2006), Calibrated radiance measurements with an air-filled glow discharge tube: Application to sprites in the mesosphere, in *Sprites, Elves and Intense Lightning Discharges*, *NATO Sci. Ser., Ser. II*, vol. 225, edited by M. Füllekrug, E. A. Mareev, and M. J. Rycroft, p. 237, Springer, Dordrecht, Netherlands.

F. J. Gordillo-Vázquez and A. Luque, Instituto de Astrofísica de Andalucía, CSIC, PO Box 3004, E-18080 Granada, Spain. (vazquez@iaa.es; aluque@iaa.es)